

Characteristics analysis of hybrid ZSM-5 zeolite catalyst with nano $\text{La}_2\text{Zr}_2\text{O}_7$ for ammonia-selective catalytic reduction (NH_3 -SCR) of NO_x

M. Sunil Kumar*, M. S. Alphin, S. A. Srinivasan, S. Vignesh, T Subash
Department of Mechanical Engineering, Sri Sivasubramaniya Nadar College of Engineering, Kalavakkam, Chennai, Tamil Nadu, India – 603110

The characteristic effects of ZSM-5 by doping $\text{La}_2\text{Zr}_2\text{O}_7$ nanoparticle was investigated based on the application of ammonia-selective catalytic reduction (NH_3 -SCR). The hybrid ZSM-5 zeolite catalyst was synthesized by the Ion exchange and wet impregnation method to develop Cu-ZSM-5 and 5%, 10%, & 15% of $\text{La}_2\text{Zr}_2\text{O}_7$ based Cu-ZSM-5. The characterization of hybrid catalyst was analysed by XRD, SEM, XPS, BET, FT-IR, & UV-Vis. From the analysis of the characteristics, $\text{La}_2\text{Zr}_2\text{O}_7$ doped Cu-ZSM-5 hybrid zeolite catalyst exhibits excellent properties towards the application of ammonia-selective catalytic reduction (NH_3 -SCR) for the reduction of oxides of nitrogen to achieve EURO VI norms.

(Received August 22, 2022; Accepted December 8, 2022)

Keywords: Zeolite, Ammonia-selective catalytic reduction, Nanoparticle, Emission, Characteristics

1. Introduction

A slew of environmental problems arises due to the increased usage of stationary and mobile vehicles emitting a huge amount of NO_x ($X = 1, 2$), which doesn't satisfy EURO VI norms [1]–[3]. To achieve norms and to reduce slay of environmental problems, several researchers developed technology for NO_x disposal has been developed as selective and non-selective catalytic reduction, and selective non-catalytic reduction, and photocatalysis, among SCR with NH_3 as a reducing agent has promising results for reduction of NO_x due to broadened operating temperature window with high selectivity of N_2 [4]–[6].

In recent decades iron and copper doped zeolites (Cu-Z & Fe-Z) have attracted much interest as a catalyst for reducing NO_x in post-treatment technology. But, Fe-Z was not appreciable for a low operating temperature window than Cu-Z because Cu^{2+} occupies the ellipsoidal cavity in the zeolite structure [7]. In addition, the preparation method also plays a vital role as ion exchange of Cu in H-ZSM zeolite has a greater number of isolated Cu ions than precipitation of Cu in H-ZSM. Along with highly ZSM-5 catalyst was highly influenced towards NH_3 -SCR activity due to increased pair of Cu^{2+} concentration and specific activity because Cu^{2+} species acts as an active species for NH_3 -SCR activity [8].

CeO_2 has recently received much prominence because of its storage capacity of oxygen and outstanding reduction-oxidation characteristics [9]. Ce-catalysts' NO_x conversion displays over 90% NO_x reduction when utilized as supports or promoters, and active species at temperatures ranging from 250 to 450°C. This catalytic system, however, is extremely vulnerable to SO_2 poisoning. Cerium oxygen species on the surface unavoidably combine with sulfur dioxide to create $\text{Ce}_2(\text{SO}_4)_3$ or $\text{Ce}(\text{SO}_4)_2$, explains why the catalysts have decreased activity during the SO_2 deactivation phase and is the most significant barrier to the industrialisation of CeO_2 -based catalysts in SCR systems [10], [11]. But the combination of Cr and CeO_2 in ZSM-5 zeolite may provide a broad window of operating temperature, and improved SO_2 resistance due to the variety of chromium oxidation states such as Cr(VI) and Cr(III), providing an interaction with acidic

* Corresponding author: sunil240697@gmail.com
<https://doi.org/10.15251/DJNB.2022.174.1423>

strength of ZSM-5 to increase the NH_3 -SCR activity against CH_3SH [12], [13]. Similarly, as reported previously, a variety of Ce oxidation states Ce(IV), and Ce(III) entailed a reversible redox cycle which is beneficial against CH_3SH activity. So, chromium species will promote catalytic activity due to its high redox characteristics of Cr(VI) as an active site and stable structure of the zeolite can be held by the addition of lanthanum, and it also generates more vacancies of oxygen which helps for catalytic activity. Zr-based materials have some practical advantages, such as non-toxicity, acidity, high-temperature phase stability, and redox characteristics [14], [15]. On the other hand, these catalysts have either been evaluated using particle shape or assessed almost at low GHSV of $10,000 \text{ h}^{-1}$. These settings are not feasible since the shape of the catalyst and the GHSV characteristics are two of the most crucial influencing variables on NH_3 -SCR performance [16]. Because of its short diffusion distance, low-pressure drop, and huge geometric surface area, monolith catalysts are typically more proximate to actual application. As a result, it is vital to build monolithic acidic zirconium-based composite oxide catalysts with hydrothermal stability and high resistance to space velocity [17]. Recent research has demonstrated the feasibility of using REE compounds in the catalyst composition [18].

We now investigate the characteristic effects of lanthanum zirconate ($\text{La}_2\text{Zr}_2\text{O}_7$) over the doping of Cu-ZSM-5, a hybrid zeolite catalyst for ammonia-selective catalytic reduction (NH_3 -SCR) of NO_x by XRD, SEM, XPS, BET, FT-IR, & UV-Vis.

2. Catalyst preparation

The chemical ion exchange method and wet impregnation method were used to prepare a hybrid ZSM-5 zeolite catalyst. Cupric nitrate was used as a precursor for Cu species, and ZSM-5 zeolite, Lanthanum oxide (La_2O_3), Zirconium (ZrO_2) was purchased from ZR catalyst, Rare Earth India, and Loba chemicals, respectively. Lanthanum Zirconate ($\text{La}_2\text{Zr}_2\text{O}_7$) was synthesized by the molten salt method with a molar ratio of 1:2 between La_2O_3 : ZrO_2 [19].

Initially, the ion exchange process was done to synthesize Cu-ZSM-5 catalyst by 0.02M of 320mL solution with constant stirring for a day, and then filtered and washed with deionized water and kept at 110°C for drying a day to ensure the complete ion exchange of Cu in ZSM-5, the process is repeated and final sample as Cu-ZSM-5 zeolite catalyst. Then, wet impregnation of $\text{La}_2\text{Zr}_2\text{O}_7$ and Cu-ZSM-5 zeolite catalyst began at a wt.% of 5, 10, and 15 between them. Cu-ZSM-5 and $\text{La}_2\text{Zr}_2\text{O}_7$ dispersed on ethanol separately and sonicated for 30mins and mixed for sonication of 90 mins along with magnetic stirring for 90mins. After this, they were kept for drying at 120°C for 150 mins and then allowed to dry at room temperature overnight. The prepared catalyst was kept for calcination at a temperature of 500°C for 4hrs and cooled to room temperature. Prepared catalyst was crushed and sieved for further experimentation purposes as mentioned as $5\text{La}_2\text{Zr}_2\text{O}_7/\text{Cu-ZSM-5}$, $10\text{La}_2\text{Zr}_2\text{O}_7/\text{Cu-ZSM-5}$, & $15\text{La}_2\text{Zr}_2\text{O}_7/\text{Cu-ZSM-5}$ for 5, 10, & 15 wt.% of $\text{La}_2\text{Zr}_2\text{O}_7$ and Cu-ZSM-5.

3. Catalyst characterization

The wet-impregnation catalyst was characterised using the following techniques: an ASAP2020 physical absorber was used to assess pore diameter, pore volume, and Brunauer-Emmett-Teller (BET) surface area. X-ray diffraction (XRD) and scanning electron microscopy (SEM) were utilised to describe XRD spectra obtained using Cu K_α radiation at 40 mA and 45 kV with a scanning angle (2θ) of $5^\circ - 90^\circ$, as well as dispersion and morphological features of the catalyst. Using Al K_α radiation in X-ray photoelectron spectroscopy, catalysts were evaluated for their chemical state and elemental composition (XPS). The functional group and absorbance of the catalyst were determined using FT-IR (PerkinElmer Spectrum Two) and UV-Vis spectroscopy (JASCO V-780) over a range of $4000 - 400 \text{ cm}^{-1}$ with a resolution of 1cm^{-1} and $1100 - 200\text{nm}$ with a precision of -0.2nm .

4. Results and discussion

4.1 XRD analysis

Zeolite and its hybrid catalyst are analyzed for crystallinity and purity of its phases using X-ray diffraction spectrometer analysis given in fig.1. From fig.1 indicating that diffraction peaks of typical MFI ZSM-5 zeolite $2\theta = 22.5^\circ$, 24.0° , & 29.8° were observed in ZSM-5 pattern [5], [20]. As the ion exchange process of Cu was done, the intensity of peaks gets reduced due to the ion exchange of Cu, indicating that the molar ratio of SAR decreases [21]. The diffraction pattern of $\text{La}_2\text{Zr}_2\text{O}_7$ was observed in a hybrid catalyst with no formation of hydrates and impurities. Still, MFI ZSM-5 peak intensity gets reduced due to doping of $\text{La}_2\text{Zr}_2\text{O}_7$, indicating pattern reduction of SAR ratio. In $2\theta = 35^\circ$ to 45° , the diffraction peaks of $\text{La}_2\text{Zr}_2\text{O}_7$ match the ICDD pattern (ICDD: 09-8441) [19]. As the doping percentage of $\text{La}_2\text{Zr}_2\text{O}_7$ increases, their respective peaks' intensity increases. As a result, the impure phase was not detected, indicating its crystallinity nature and phase purity of the sample. All samples exhibit pure MFI ZSM-5 peaks, and all hybrid zeolites exhibit $\text{La}_2\text{Zr}_2\text{O}_7$ peaks proportional as the percentage increases its intensity.

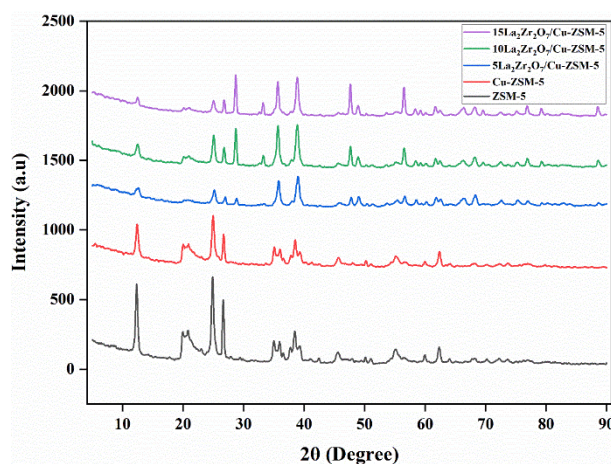


Fig. 1. XRD pattern of ZSM-5 and its hybrid catalyst.

4.2. SEM analysis

The morphological characteristics of ZSM-5, Cu-ZSM-5, and $\text{La}_2\text{Zr}_2\text{O}_7/\text{Cu-ZSM-5}$ were shown in fig.2. Fig 2 a) shows the morphology of ZSM-5, which exhibits cubic structure and as doping of Cu i.e., Cu^{2+} ion over ZSM-5 exhibits as a same cubic structure without any high modification in its morphology which shows Cu doping doesn't ZSM-5 crystalline structure and stability shown in fig.2 b). Fig.2c) shows the morphology of $\text{La}_2\text{Zr}_2\text{O}_7$ nanoparticles, exhibiting both irregular and regular polyhedral structures. The particle size is directly influenced by the growth mechanism [19]. The morphology of the hybrid catalyst $\text{La}_2\text{Zr}_2\text{O}_7/\text{Cu-ZSM-5}$ is shown in Fig.2 d), which exhibits both cubic and regular & irregular polyhedral shapes. It indicates that all the species, such as Cu and $\text{La}_2\text{Zr}_2\text{O}_7$ were well dispersed over the ZSM-5 zeolite. Fig.2 indicates that there is no formation of agglomeration and ZSM-5 structure exhibited in all the catalysts i.e. in Cu-ZSM-5 and $\text{La}_2\text{Zr}_2\text{O}_7/\text{Cu-ZSM-5}$.

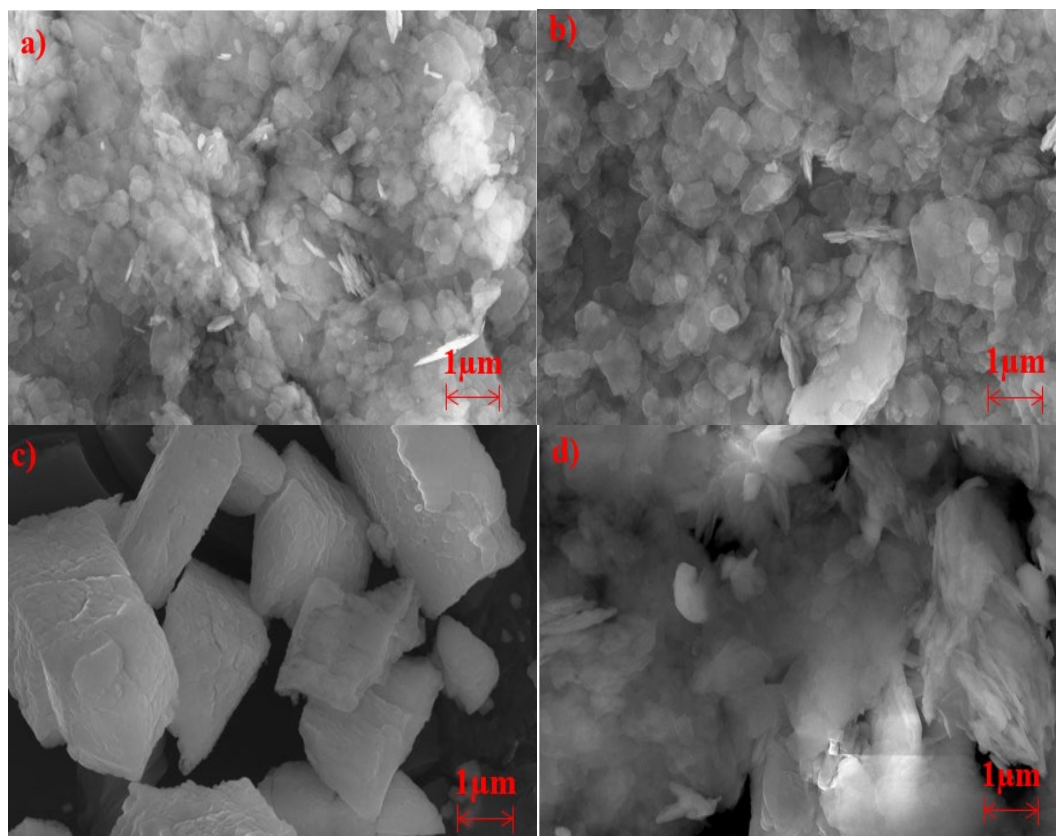


Fig. 2. SEM images of a) ZSM-5, b) Cu-ZSM, c) $\text{La}_2\text{Zr}_2\text{O}_7$, & d) $\text{La}_2\text{Zr}_2\text{O}_7/\text{Cu-ZSM-5}$ catalyst.

4.3. BET analysis

Zeolite and hybrid zeolite catalyst analysis for pore volume, pore size, and surface area shown in table 1. The BET surface area of ZSM-5 zeolite was $415.231\text{m}^2/\text{g}$. In addition of Cu species over ZSM-5 zeolite, the surface area gets reduced without affecting crystallinity to illustrate the SCR activity. The surface area for hybrid zeolite catalyst was reduced inversely as the percentage of doping of nanomaterial $\text{La}_2\text{Zr}_2\text{O}_7$. As increasing $\text{La}_2\text{Zr}_2\text{O}_7$ weight percentage with ZSM-5 zeolite, the surface area gets reduced due to doping over the surface of ZSM-5. But, still, the reduction of surface area was not influenced much by the catalytic activity of SCR [3], [6] because catalytic activity was highly influenced by the strength of active sites and nature of active sites, which can be influenced by doping of Cu, and $\text{La}_2\text{Zr}_2\text{O}_7$ over ZSM-5 to increase the activity of SCR.

Table 1. Properties of catalyst.

Sample	S_{BET} (m^2/g)	Pore Volume (cm^3/g)	Average Pore Size (nm)
ZSM-5	415.231	0.187	2.09
Cu-ZSM-5	349.721	0.133	2.11
5 $\text{La}_2\text{Zr}_2\text{O}_7/$ Cu-ZSM-5	271.414	0.109	2.19
10 $\text{La}_2\text{Zr}_2\text{O}_7/$ Cu-ZSM-5	268.635	0.104	2.23
15 $\text{La}_2\text{Zr}_2\text{O}_7/$ Cu-ZSM-5	259.263	0.101	2.25

4.4. FT-IR analysis

FT-IR spectra for both ZSM-5 and its hybrid zeolite catalyst were analysed to define its functional groups shown in fig.3. From fig.3, a range 1100cm^{-1} and 540cm^{-1} refers to a typical MFI

ZSM-5 [22] structure due to asymmetric vibration of stretching and bending of insensitive internal tetrahedron. In contrast, characteristic band of MFI ZSM-5 at 620cm^{-1} was observed in all the catalyst prepared represents the degree of crystallinity [23]. Structure sensitive and insensitive exterior and internal tetrahedron symmetric stretching vibrations are responsible for the band at 800cm^{-1} . MFI ZSM-5 zeolite catalyst has sub nanocrystal in primary structure at 620cm^{-1} , which is weak. For Cu-ZSM-5 catalyst, characteristic band intensity gets reduced than ZSM-5 due to addition of Cu which influence in SAR ratio and then band in-between $2500\text{-}2000\text{cm}^{-1}$ refers to vibration of Zr-O due to stretching of C=C refers high stable Zr-O and band between $1500\text{-}1000\text{cm}^{-1}$ refers to La-O ionic vibrations due to bending band of C-H at 1481cm^{-1} . Finally, the band $< 1000\text{cm}^{-1}$ refers to La-O-Zr because of the bending of C-H [19]. From these bands, hybrid zeolite catalyst exhibits excellent crystallinity with no impure phase formation with ZSM-5 tends to a wide application in SCR catalytic activity.

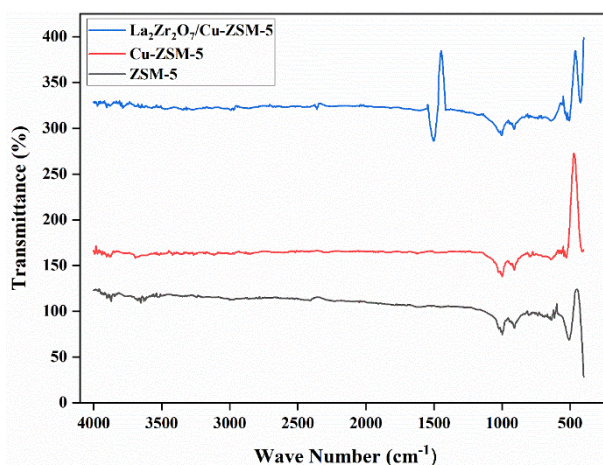


Fig. 3. FT-IR spectra of ZSM-5 and its hybrid catalyst.

4.5. UV-Vis analysis

Absorbance spectra of UV-Vis for the catalyst ZSM-5, Cu-ZSM-5, and $\text{La}_2\text{Zr}_2\text{O}_7/\text{Cu-ZSM-5}$ were shown in fig.4. The band of adsorption as 210nm & 280nm refers to ZSM-5 zeolite catalyst [24], [25]. The intensity of the ZSM-5 zeolite band gets reduced for Cu-ZSM-5 due to doping of Cu species over the ZSM-5 catalyst. Initially, band can be assigned to isolated Cu^{2+} ion due to O to Cu transition in coordination with lattice oxygen, whereas later Cu^{2+} ion is assigned to d-d transition due to CuO crystalline distribution in an octahedral coordinate on the catalyst surface [26]. When $\text{La}_2\text{Zr}_2\text{O}_7$ was added to Cu-ZSM-5, another band was observed.

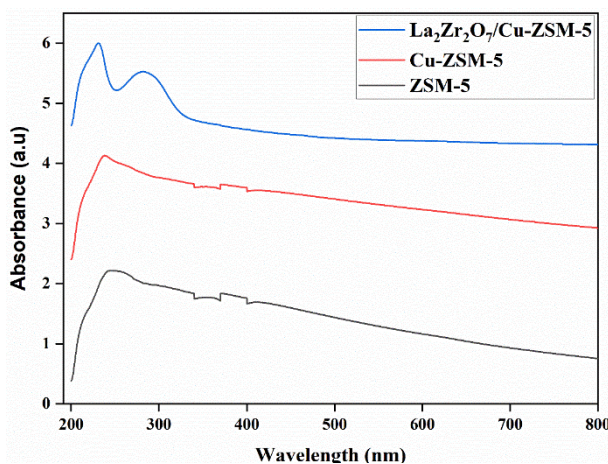


Fig. 4. UV-Vis spectra of ZSM-5 and its hybrid catalyst.

The observed band at 300nm illustrates the presence of two groups La^{3+} and Zr^{4+} , which is more advantageous for SCR activity [27]. Similarly, the ZSM-5 absorbance band was observed in $\text{La}_2\text{Zr}_2\text{O}_7/\text{Cu-ZSM-5}$, which illustrates that lanthanum zirconate nanoparticle doesn't affect the crystalline structure of ZSM-5 zeolite and attributes to phase purity of ZSM-5 with well disperse over the surface of Cu-ZSM-5 catalyst.

4.6. XPS analysis

The spectra of Cu^{2+} , La^{3+} , and Zr^{4+} doped on ZSM-5 catalyst were observed by XPS spectra in fig.5. Fig.5 A) shows XPS spectra of Cu^{2+} for Cu-ZSM-5 catalyst, which Cu^{2+} exhibits in two forms as $\text{Cu } 2p_{3/2}$ & $2p_{1/2}$ with their binding energies of 932.5 & 952.3 eV respectively [28]. Then fig.5 b) shows XPS spectra of La^{3+} and Zr^{4+} of $\text{La}_2\text{Zr}_2\text{O}_7/\text{Cu-ZSM-5}$ catalyst. The binding energy values for $\text{Zr } 3d_{5/2}$ & $3d_{3/2}$ are 181.7 & 185.2 eV, respectively, in the $\text{Zr } 3d$ spectrum [29]. These findings show that Zr^{4+} ions replace in the ZSM-5 catalyst structure. Peaks in the $\text{La } 3d$ spectrum have binding energies of 835 and 852 eV for $\text{La } 3d_{5/2}$ and $\text{La } 3d_{3/2}$.

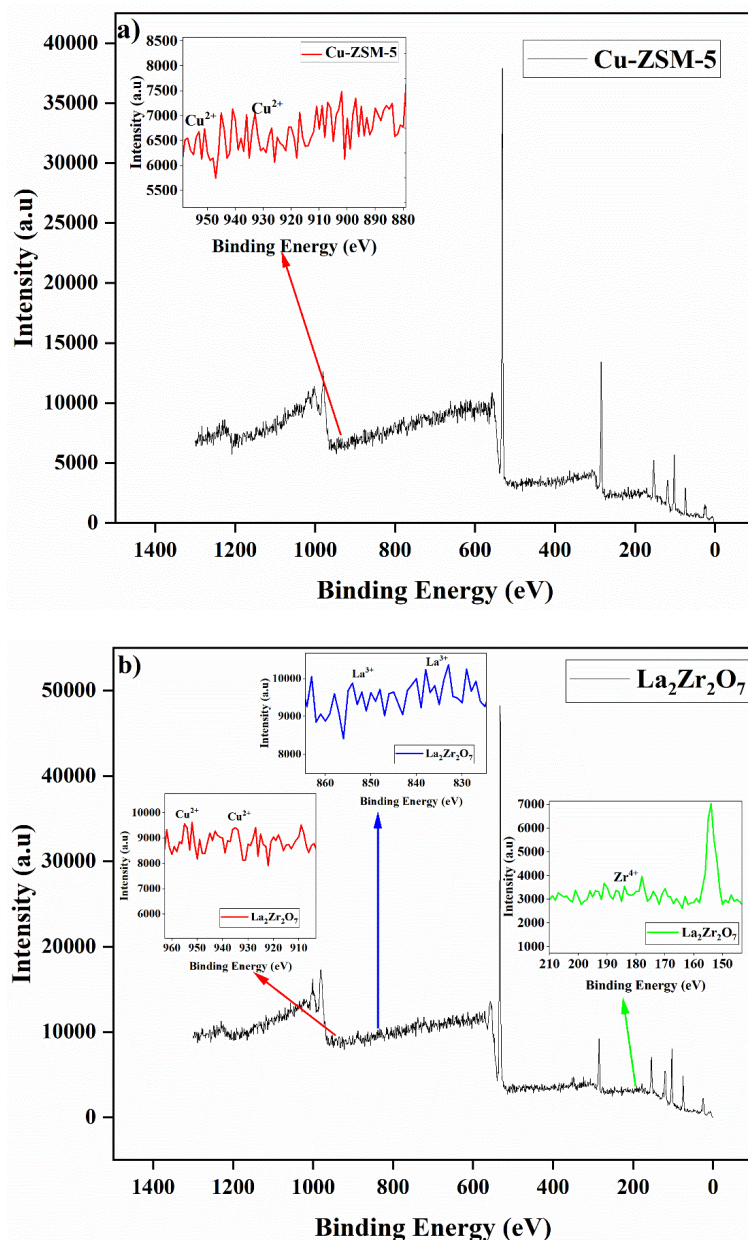


Fig. 5. XPS spectra of the hybrid catalyst a) Cu-ZSM-5, & b) $\text{La}_2\text{Zr}_2\text{O}_7/\text{Cu-ZSM-5}$.

According to the La 3d spectrum results, lanthanum resides in the +3 state in La³⁺ doped ZSM-5. Furthermore, when compared to the conventional XPS energy peak of La 3d in La₂O₃, the peak for La 3d spectrum in La³⁺ doped ZSM-5 shows a modest chemical shift to low binding energy. When compared to pure La₂O₃, this is due to changes in the chemical environment of La³⁺ and the distance between lanthanum and oxygen [30]. Because of their high oxidation and reduction properties, these existing states of catalyst Cu-ZSM-5 and La₂Zr₂O₇/Cu-ZSM-5, such as Cu²⁺, La³⁺, and Zr⁴⁺ will have a greater influence on SCR catalytic activity [31].

5. Conclusion

The characteristics effects of hybrid catalyst such as Cu-ZSM-5 and La₂Zr₂O₇/Cu-ZSM-5 was analysed with reference to ZSM-5 catalyst in which Cu-ZSM-5 was prepared by ion exchange of Cu with ZSM-5 catalyst and La₂Zr₂O₇/Cu-ZSM-5 catalyst was prepared by wet impregnation of La₂Zr₂O₇ and Cu-ZSM-5 with wt.% of 5, 10, and 15%. The prepared catalyst was analysed by XRD, SEM, BET, FT-IR, UV-Vis, and XPS characterization. As a result from characterization it states that La₂Zr₂O₇/Cu-ZSM-5 has wide application in ammonia-selective catalytic reduction (NH₃-SCR) activity due to high crystallinity nature with no impurities and agglomeration defined by XRD pattern along with a high surface area of 259.263 m²/g, but still, the surface area was reduced due to doping of Cu, La, and Zr species over the parental ZSM-5 defined by BET analysis but the surface area doesn't affect NH₃-SCR activity. In addition, FT-IR and UV-Vis define their presence and functional group of doped species without any disturbance in the original structure and presence of impure phase in ZSM-5, and finally XPS spectra state their ionic state in which Cu²⁺, La³⁺, and Zr⁴⁺ exhibits in the binding energies of 932.5 & 952.3 eV as Cu 2p_{3/2} and Cu 2p_{1/2}, 835 & 852 eV as La 3d_{5/2} and La 3d_{3/2}, and 181.7 & 185.2 eV as Zr 3d_{5/2} and Zr 3d_{3/2} respectively indicates La₂Zr₂O₇/Cu-ZSM-5 has high application in ammonia-selective catalytic reduction (NH₃-SCR) activity due to high redox property.

References

- [1] Y. Devarajan, B. Nagappan, G. Mageshwaran, M. Sunil Kumar, R. B. Durairaj, *Fuel*, 277 (2020); <https://doi.org/10.1016/j.fuel.2020.118161>
- [2] M. S. Kumar M. S. Alphin, *Reaction Kinetics, Mechanisms and Catalysis* (2022).
- [3] S. Raja, M. S. Alphin, *Reaction Kinetics, Mechanisms and Catalysis* 129(2), 787-804 (2020); <https://doi.org/10.1007/s11144-020-01735-6>
- [4] S. Raja, M. S. Alphin, L. Sivachandiran, *Catalysis Science & Technology* 10(23), 7795-7813 (2020); <https://doi.org/10.1039/D0CY01348J>
- [5] J. Ding et al., *Catalysis Today* 384-386, 106-12 (2022); <https://doi.org/10.1016/j.cattod.2021.05.013>
- [6] S. Raja, M. S. Alphin, *Journal of Nanoparticle Research* 22(7), 190 (2020); <https://doi.org/10.1007/s11051-020-04919-2>
- [7] Y. Wang, X. Ji, H. Meng, L. Qu, X. Wu, *Catalysis Communications* 138, 105969 (2020); <https://doi.org/10.1016/j.catcom.2020.105969>
- [8] C. Peng et al., *Journal of Hazardous Materials* 385, 121593 (2020); <https://doi.org/10.1016/j.jhazmat.2019.121593>
- [9] H. He et al., *Ceramics International* 42(6), 7810-18 (2016); <https://doi.org/10.1016/j.ceramint.2016.02.005>
- [10] T. Boningari, A. Somogyvari, P. G. Smirniotis, *Industrial & Engineering Chemistry Research* 56(19), 5483-94 (2017); <https://doi.org/10.1021/acs.iecr.7b00045>
- [11] D. Damma, T. Boningari, P. G. Smirniotis, *Molecular Catalysis* 451, 20-32 (2018); <https://doi.org/10.1016/j.mcat.2017.10.013>
- [12] C. Cammarano, E. Huguet, R. Cadours, C. Leroi, B. Coq, V. Hulea, *Applied Catalysis B*:

- Environmental 156-157, 128-33 (2014); <https://doi.org/10.1016/j.apcatb.2014.03.026>
- [13] J. Yu et al., *Materials Chemistry and Physics* 239, 121952 (2020); <https://doi.org/10.1016/j.matchemphys.2019.121952>
- [14] H. Xu et al., *Chinese Journal of Catalysis* 33(11), 1927-37 (2012); [https://doi.org/10.1016/S1872-2067\(11\)60467-1](https://doi.org/10.1016/S1872-2067(11)60467-1)
- [15] N. Marcotte et al., *Applied Catalysis B: Environmental* 105(3), 373-76 (2011); <https://doi.org/10.1016/j.apcatb.2011.04.022>
- [16] P. Granger, V. I. Parvulescu, *Chemical Reviews* 111(5), 3155-3207 (2011); <https://doi.org/10.1021/cr100168g>
- [17] P. I. Kyrriienko et al., *Molecular Catalysis* 518, 112096 (2022); <https://doi.org/10.1016/j.mcat.2021.112096>
- [18] W. Zhang et al., *Catalysis Science & Technology* 12(8), 2566-77 (2022).
- [19] S. A. Srinivasan, S. P. Kumaresh babu, L. John Berchmans, M. Usmaniya, *Materials Research Express* 6(10), 104001 (2019); <https://doi.org/10.1088/2053-1591/ab3683>
- [20] M. Liu et al., *RSC Advances* 5(12), 9237-40 (2015); <https://doi.org/10.1039/C4RA14955F>
- [21] T. Qiao, Z. Liu, C. Liu, W. Meng, H. Sun, Y. Lu, *Applied Catalysis A: General* 617, 118128 (2021); <https://doi.org/10.1016/j.apcata.2021.118128>
- [22] I. Ali, A. Hassan, S. Shabaan, K. El-Nasser, *Arabian Journal of Chemistry* 10, S2106-14 (2017); <https://doi.org/10.1016/j.arabjc.2013.07.042>
- [23] O. Ben Mya, M. Bitu, I. Louafi, A. Djouadi, *MethodsX* 5, 277-82 (2018). <https://doi.org/10.1016/j.mex.2018.03.004>
- [24] M. H. Groothaert, J. A. van Bokhoven, A. A. Battiston, B. M. Weckhuysen, R. A. Schoonheydt, *Journal of the American Chemical Society* 125(25), 7629-40 (2003); <https://doi.org/10.1021/ja029684w>
- [25] S. Yashnik, Z. Ismagilov, *Applied Catalysis B: Environmental* 170-171, 241-54 (2015); <https://doi.org/10.1016/j.apcatb.2015.01.021>
- [26] S. Lai et al., *RSC Adv* 5(110), 90235-44 (2015); <https://doi.org/10.1039/C5RA12505G>
- [27] K. V Tenorio et al., *Thermochimica Acta* 690, 178662 (2020); <https://doi.org/10.1016/j.tca.2020.178662>
- [28] H. Wang, R. Xu, Y. Jin, R. Zhang, *Catalysis Today* 327, 295-307 (2019); <https://doi.org/10.1016/j.cattod.2018.04.035>
- [29] J. C. Yu, J. Lin, R. W. M. Kwok, *The Journal of Physical Chemistry B* 102(26), 5094-98 (1998); <https://doi.org/10.1021/jp980332e>
- [30] E. R. Leite et al., *Advanced Materials* 14(12), 905-8 (2002); [https://doi.org/10.1002/1521-4095\(20020618\)14:12<905::AID-ADMA905>3.0.CO;2-D](https://doi.org/10.1002/1521-4095(20020618)14:12<905::AID-ADMA905>3.0.CO;2-D)
- [31] M. S. Kumar, M. S. Alphin, *Digest Journal of Nanomaterials and Biostructures* 17(4), 1313-1325 (2022); <https://doi.org/10.15251/DJNB.2022.174.1313>